


## Covalent Organic Frameworks with High Charge Carrier Mobility

Shun Wan,<sup>†</sup> Felipe Gándara,<sup>†</sup> Atsushi Asano,<sup>‡</sup> Hiroyasu Furukawa,<sup>†</sup> Akinori Saeki,<sup>‡</sup> Sanjeev K. Dey,<sup>§</sup> Lei Liao,<sup>†</sup> Michael W. Ambrogio,<sup>§</sup> Youssry Y. Botros,<sup>§,¶,||</sup> Xiangfeng Duan,<sup>†</sup> Shu Seki,<sup>‡</sup> J. Fraser Stoddart,<sup>§</sup> and Omar M. Yaghi<sup>\*,†,⊥</sup><sup>†</sup>Department of Chemistry and Biochemistry, University of California, Los Angeles, California 90095, United States<sup>‡</sup>Department of Applied Chemistry, Graduate School of Engineering, Osaka University, 2-1 Yamadaoka, Suita, Osaka 565-0871, Japan, and PRESTO, JST, Japan<sup>§</sup>Center for the Chemistry of Integrated Systems, Department of Chemistry, and Department of Material Science and Engineering, Northwestern University, 2145 Sheridan Road, Evanston, Illinois 60208, United States<sup>¶</sup>Intel Laboratories, Santa Clara, California 95054-1549, United States<sup>||</sup>National Center for Nano Technology Research, King Abdulaziz City for Science and Technology (KACST), Riyadh, 11442, Kingdom of Saudi Arabia<sup>⊥</sup>Center for Reticular Chemistry, Center for Global Mentoring, UCLA-DOE Institute for Genomics and Proteomics, University of California-Los Angeles, 607 Charles E. Young Drive East, Los Angeles, California 90095, United States Supporting Information**KEYWORDS:** covalent organic frameworks, charge carrier mobility, porphyrin, porous materials

Conductive organic materials are important because of their interesting electronic and optoelectronic properties, low cost and weight, and the ease with which they can be fabricated. Their mechanical flexibility has opened up new applications such as flexible displays.<sup>1</sup> An important characteristic of a semiconductor is the ability to control its electrical conductance, where the most important property, characterizing the charge transport ability, is the charge carrier mobility,<sup>2</sup>  $\mu$ . It is widely believed that strong cofacial interactions between polymer chains allow for charge carriers to be transported easily from one chain to another.<sup>3</sup> However, linear polymers have only confined lateral overlap, and materials with large intermolecular conduction cross-sections have thus far remained a difficult challenge to construct.

To enhance the mobility of charge carriers in organic semiconductors, highly crystalline structures with close interactions between internal segments are essential design features.<sup>4</sup> Very rarely have one-dimensional polymers shown high charge carrier mobility values;<sup>5</sup> however, most of these compounds typically exhibit<sup>3,6</sup> small and limited overlap between “slim” backbones, even in the face-to-face stacking mode. Therefore two-dimensional (2D) flat sheet structures constitute an ideal morphology from the viewpoint of maximizing intermolecular interactions. Such interactions take place when all the atoms within the structure are completely superimposed upon those of the neighboring sheet. These assemblages should create a broad path for charge carriers moving from one sheet to another, enabling the eclipsed integration of  $\pi$ -electronic components into a well-defined 2D layered framework.

Covalent organic frameworks (COFs) are a class of porous crystalline materials constructed by the linkage of organic secondary building units (SBUs) through covalent bonds to produce predetermined structures. The topology of the frameworks obtained is imposed by the geometrical features of the

SBUs, according to the principles of reticular chemistry.<sup>7</sup> Within the COF class of materials, both three-dimensional (3D) structures and 2D layered materials are prepared, depending on the degree of connectivity and geometry of the selected organic building units.<sup>8</sup> Materials belonging to the 2D COFs subclass with desirable properties have been prepared by the stacking of organic layers. These materials feature a variety of pore sizes and high surface areas and their usefulness for the storage of gases<sup>9</sup> such as H<sub>2</sub> and NH<sub>3</sub> has been demonstrated. Remarkably, in these 2D structures, we have observed shortened interlayer distances,<sup>8a,b</sup> suggesting the existence of interactions between the aromatic organic components of the layers. Ideally, a 2D COF with a  $\pi$ -conjugated system and short interlayer distances could exhibit electronic interactions between the different sheets, and hence potentially become a conductive material.<sup>10</sup>

With this background in mind, we designed two new 2D COFs, each with a  $\pi$ -conjugated system, with the expectation that their short interlayer distances would allow for electronic interactions between the different sheets. Accordingly, we have selected porphyrin units with the aim of creating an extended planar  $\pi$ -electron system that allows close intermolecular  $\pi$ - $\pi$  distances, resulting (Scheme 1) in the formation of two new COFs (COF-366 and -66) with the highest charge carrier mobility values among known organic crystalline conducting polymers.

Both COFs were synthesized by solvothermal reactions (See the Supporting Information). In the case of COF-366, the formation of the imine bond between the porphyrin and the terephthaldehyde was confirmed by FT-IR and <sup>13</sup>C cross-polarization with

Received: April 21, 2011

Revised: July 26, 2011

Published: August 22, 2011

**Scheme 1. Condensation Reactions between TAPP and Terephthalaldehyde, TBPP, and THAn Produce Extended (a) COF-366 and (b) COF-66**

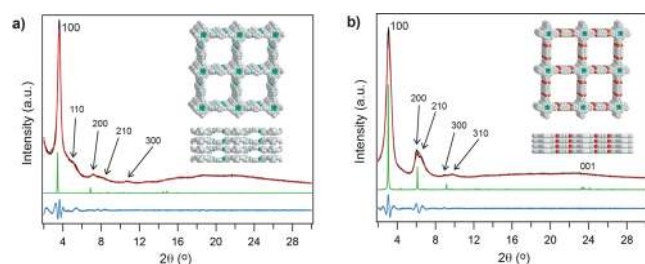
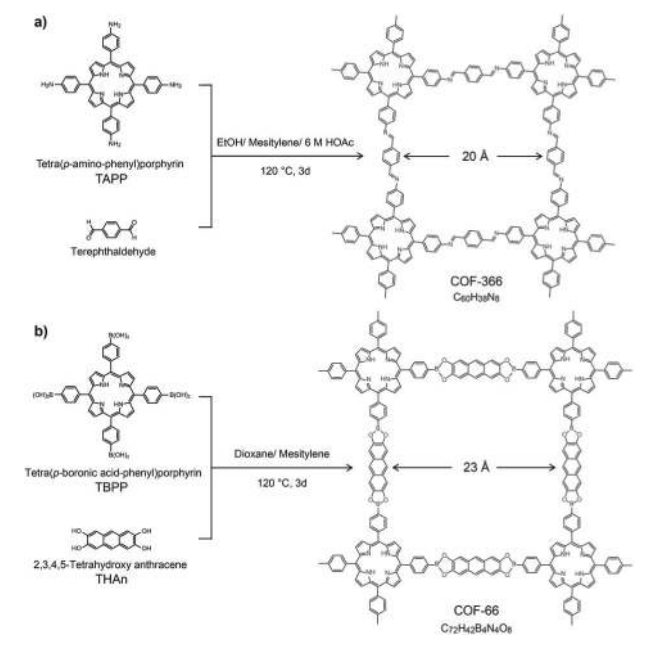


**Figure 1.** PXRD study of (a) COF-366 and (b) COF-66 with the observed pattern in black, the refined profile in red, and the difference plot in blue (observed minus refined profiles). The calculated PXRD pattern from the proposed models is shown in green. Inset: Structural representation of COFs based on powder diffraction and modeling projected along the *c* axis (top) and the *b* axis (bottom) (H atoms are omitted). C, N, B, and O are represented in turn as gray, green, yellow and red spheres.

magic-angle spinning (CP-MAS) NMR spectroscopic techniques. The FT-IR spectrum clearly reveals the C=N stretching of imine functions ( $\nu_{\text{C=N}} = 1620$  and  $1249 \text{ cm}^{-1}$ ),<sup>8d</sup> whereas the  $^{13}\text{C}$  CP-MAS NMR spectrum has a resonance at 156.95 ppm for the carbon of the C=N bond, a 2 ppm shift from the resonance observed for the carbon adjacent to the amino group of the TAPP linker. In the case of COF-66, spectroscopic data (FT-IR,  $^{11}\text{B}$ , and  $^{13}\text{C}$  MAS NMR) were similar to those performed on the reported COFs<sup>8a,b</sup> of the microcrystalline powder, which is indicative of the formation of  $\text{C}_2\text{O}_2\text{B}$  rings (see the Supporting Information).

Powder X-ray diffraction (PXRD) patterns of the two COFs demonstrate their crystalline nature (Figure 1). In both cases, a strong diffraction peak appears at a low angle, characteristic of the expected large unit-cell parameters,  $2\theta = 3.0$  and  $3.5^\circ$  for COF-66 and -366, respectively, along with some other peaks with lower diffraction intensities. No diffraction peaks appeared that were

characteristic of the starting materials. The peaks are relatively broad, which is attributed to strain defects of the perfect lattice, and/or particle size effects.

To elucidate the lattice packing, we constructed crystal models using *Materials Studio* software package (see the Supporting Information, Section S3). The square geometry of the porphyrin unit suggests the formation of square layers. Accordingly, modeling was performed in the tetragonal system, with layers lying on the *ab* plane. Two extreme possibilities were evaluated, with respect to the stacking of the layers: (i) a fully eclipsed model with an AA stacking sequence, and (ii) a staggered model with an AB stacking sequence of layers, each layer translated from the next one by one-half of the *a* and *b* lattice parameters. These two models were constructed in the space groups  $P4/mmm$  and  $I4/mmm$  for COF-66, and in the space groups  $P4/m$  and  $I4/m$  for COF-366. A geometrical energy minimization was performed using the universal force-field to optimize the geometry of the building molecules and the unit-cell parameters. When the PXRDs for the models were calculated and compared with the experimental ones, we observed excellent agreement with the fully eclipsed model in the case of both materials. A full profile pattern matching (Pawley) refinement was subsequently carried out to determine the unit cell parameters for both structures, obtaining good agreement factors in the case of both compounds. Therefore, on the basis of these results, we consider the materials as being composed of square layers, stacking along the 001 direction with interlayer distances between the centroids of the stacked porphyrin units of 5.64 and 3.81 Å for COF-366 and -66, respectively. Hollow channels are produced, running along the *c* axis, with a diameter of 20.2 and 23.2 Å for COF-366 and -66 (Figure 1), respectively, as calculated using the Platon software, cavity routine.

To investigate the details of the pore characteristics, we employed Ar adsorption measurements for both COFs at 87 K. The Ar isotherms show (Figures S13, S14, and S16 in the Supporting Information) significant uptake in the low-pressure region ( $P/P_0 < 0.1$ ), an observation which is indicative of the porous character. The BET surface areas for COF-366 and -66 were calculated to be 735 and  $360 \text{ m}^2 \text{ g}^{-1}$ , respectively. Estimated total pore volumes for COF-366 and -66 are 0.32 and  $0.20 \text{ cm}^3 \text{ g}^{-1}$ , respectively. The porous structures of COF-366 and -66 were further corroborated by fitting nonlocal density functional theory models to isotherms to determine pore size distributions that are centered (17.6 and 24.9 Å) close to pore diameters obtained from the crystal structure (20.2 and 23.2 Å) (see Figures S13, S16, and S18 in the Supporting Information).

The well-defined sheet structures together with the layers alignment of COFs would benefit the flow of carriers. To verify this hypothesis, we measured the electrical conductivity of both COFs across a gap of 2  $\mu\text{m}$  between two Au electrodes. Both COFs displayed almost linear  $I-V$  profiles in air at 25 °C (Figure S21 in the Supporting Information). For example, at 0.2 V bias voltage, the electric current of COF-366 is 0.75 nA. The results prove both of the COFs are in fact conductive. Furthermore, we investigated the transient charge-carrier conduction of COF-366 and -66 by performing laser flash photolysis time-resolved microwave conductivity (FP-TRMC) measurements at 25 °C on irradiation with a 355-nm pulse laser at  $1.78 \times 10^{15}$  photons  $\text{cm}^{-2}$ . The photoinduced transient conductivity profile shows a rapid rise in current with a maximum  $\Phi\Sigma\mu$  value of  $4.1 \times 10^{-5} \text{ cm}^2 \text{ V}^{-1} \text{ s}^{-1}$  (COF-366) and  $1.7 \times 10^{-5} \text{ cm}^2 \text{ V}^{-1} \text{ s}^{-1}$  (COF-66) at a photon density of  $9.1 \times 10^{15}$  photons  $\text{cm}^{-2}$ ,

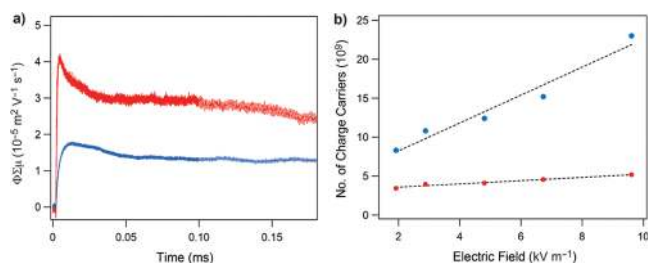


**Figure 2.** (a) FP TRMC profile of COF-366 (red) and COF-66 (blue) at 25 °C upon irradiation with a 355 nm pulse laser at a power of  $1.4 \times 10^{16}$  and  $2.1 \times 10^{16}$  photons  $\text{cm}^{-2}$ , respectively. (b) Accumulated number of photoinduced charge carriers upon 355 nm pulse exposure to COF-366 (red)/COF-66 (blue) sandwiched by ITO and Al electrodes. Excitation was carried out at the photon density of 9.

respectively (Figure 2a). To determine the numbers of photoinduced charge carriers, we integrated the time-of-flight (TOF) transient at different bias voltages (Figure 2b). The number of charge carriers were estimated via extrapolation from the bias at 0 V, to be  $3.2 \times 10^9$  (COF-66) and  $4.5 \times 10^9$  (COF-366), leading to the charge carrier generation yields  $\Phi$ , expressed as the number of charge carriers/photon of  $1.5 \times 10^{-5}$  and  $1.7 \times 10^{-5}$ , respectively. TOF transient current integration measurements performed on 1.5- $\mu\text{m}$  thick COF-366 or COF-66/poly(methyl methacrylate) films (60/40 in wt%) between Al and indium tin oxide electrodes reveal hole conduction in the case of both COFs. It transpires that COF-366 and -66 are p-type semiconductors with one-dimensional hole mobilities ( $\Sigma\mu$ ) of 8.1 and  $3.0 \text{ cm}^2 \text{ V}^{-1} \text{ s}^{-1}$ , respectively. It is generally known that the mobility values vary by changing methods. For organic field-effect transistor measurements, poly(2,5-bis(3-alkylthiophen-2-yl)thieno[3,2-*b*]thiophenes) ( $0.72 \text{ cm}^2 \text{ V}^{-1} \text{ s}^{-1}$ )<sup>5</sup> and poly(3-hexylthiophene) ( $0.1\text{--}0.5 \text{ cm}^2 \text{ V}^{-1} \text{ s}^{-1}$ )<sup>6</sup> are the two representative compounds. In the past few years, several polycrystalline polymer films have resulted in high hole mobilities of larger than  $\mu > 0.1 \text{ cm}^2 \text{ V}^{-1} \text{ s}^{-1}$  as well.<sup>11</sup> Self-assembled conjugate discotic materials, like hexaperihexabenzocoronene (HBC), a local charge carrier mobility as high as  $1.1 \text{ cm}^2 \text{ V}^{-1} \text{ s}^{-1}$  has been determined by means of the pulse-radiolysis time-resolved microwave conductivity (PR-TRMC) technique.<sup>12</sup> We emphasize that our mobilities are extraordinarily high with both values being greater than that of inorganic amorphous silicon ( $\sim 1 \text{ cm}^2 \text{ V}^{-1} \text{ s}^{-1}$ ), and much higher than those of common conjugated polymers,<sup>13</sup> thus marking COF-366 and -66 as among highest mobility, most highly ordered crystalline organic semiconductors yet known.<sup>14</sup>

Generally, single crystals perform better in charge carrier transport as a result of the slowing of the translational motion of the charge carriers at interfaces, defects, boundaries, etc. In our measurements, without the long-range translational motion of charge carriers, the mobilities of the charge carriers are consistent with those in the crystals. Given the high mobility values of ( $8.1 \text{ cm}^2 \text{ V}^{-1} \text{ s}^{-1}$ ), the electric field strength of the microwave in the cavity of the TRMC measurement ( $\sim 10 \text{ V cm}^{-1}$ ), and the turnover interval of the microwave in the cavity (9 GHz of the probing microwave and Q value of the cavity  $\sim 2500$ ), we estimate the spatial size of the oscillating motion of charge carriers in the FP-TRMC measurement as  $\sim 5 \text{ nm}$  at a maximum, which is much longer than the interlayer distances of COFs. Thus, it is presumed that the charge carrier mobility estimated by FP-TRMC should be close to the value in a single crystal, and

includes significant contribution from the local motion of charge carriers over the range of the interlayer distances. However the value of mobility determined by the conventional TOF method is more than 2 orders of magnitude lower than that by TRMC with negative dependence on the applied electric field (see Figure S28 in the Supporting Information), which shows good agreement with other organic compounds, like HBC.<sup>15</sup> This implies that the grain/domain boundaries disturb the long-range ( $\sim \mu\text{m}$ ) translational motion of charge carriers in these materials. We believe that the high-mobility carrier conduction is related to the eclipsed arrangements and  $\pi$ -conjugated intralayer structures, accounting for the higher mobility present in COF-366 compared to COF-66, and the value of TRMC mobility is responsible in the devices fabricated within nm scale.

We also found that the lifetimes of the charged species for both COFs are  $\sim 80 \mu\text{s}$  or even longer in spite of the higher mobility of the charge carriers (see Figure S26b and d in the Supporting Information). The lifetime of free charge carriers is the primary factor in the promotion of the effective charge carrier separation. Therefore, it is possible to consider fabricating a future heterojunction type solar cell based on the two COFs impressive performance on charge carrier separation.

In conclusion, two covalent organic frameworks (COFs) with structures based on covalently linked porphyrin units were synthesized. These crystalline compounds afford sheets in which the porphyrin units are stacked laterally to give an efficient conducting interface. The two porphyrin COFs (COF-366 and COF-66) were determined to be hole conducting with mobilities as high as 8.1 and  $3.0 \text{ cm}^2 \text{ V}^{-1} \text{ s}^{-1}$ . Therefore, these multifunctional conducting COFs combine thermal stability, electrical conductivity, high charge mobility, and pore accessibility, which represent an important discovery in the push to design viable plastic electronics and optoelectronic systems.

## ■ ASSOCIATED CONTENT

**S Supporting Information.** Experimental and synthesis details; complete characterization: crystallographic data, TGA, solid-state  $^{13}\text{C}$ , and  $^{11}\text{B}$  NMR; SEM images; UV-vis spectra; and additional mobility analysis. This material is available free of charge via the Internet at <http://pubs.acs.org>.

## ■ AUTHOR INFORMATION

### Corresponding Author

\*E-mail: [yaghi@chem.ucla.edu](mailto:yaghi@chem.ucla.edu).

## ■ ACKNOWLEDGMENT

The work was sponsored by U.S. Department of Energy (DE-FG36-08GO18141) and the National Center for Nano Technology Research at the King Abdulaziz City for Science and Technology (KACST) in Saudi Arabia. We thank Dr. T. M. Al-Saud and Dr. S. H. Alkhowaiter at KACST for their generous support of this program of research. F.G. acknowledges funding by the Spanish Ministry of Education (I-D+i 2008-2011).

## ■ REFERENCES

- (1) (a) Shirota, Y.; Kageyama, H. *Chem. Rev.* **2007**, *107*, 953. (b) Murphy, A. R.; Fréchet, J. M. J. *Chem. Rev.* **2007**, *107*, 1066. (c) Kulkarni, A. P.; Tonzola, C. J.; Babel, A.; Jenekhe, S. A. *Chem. Mater.* **2006**, *16*, 4556. (d) Nunzi, J.-M. C. R. *Phys.* **2002**, *3*, 523.

- (2) Laquai, F.; Wegner, G.; Bäessler, H. *Philos. Trans. R. Soc. London, Ser. A* **2007**, *365*, 1473.
- (3) Siringhaus, H.; Brown, P. J.; Friend, R. H.; Nielsen, M. M.; Bechgaard, K.; Langeveld-Voss, B. M. W.; Spiering, A. J. H.; Janssen, R. A. J.; Meijer, E. W.; Herwig, P.; de Leeuw, D. M. *Nature* **1999**, *401*, 685.
- (4) Coropceanu, V.; Cornil, J.; da Silva Filho, D. A.; Olivier, Y.; Silbey, R.; Brédas, J.-L. *Chem. Rev.* **2007**, *107*, 926.
- (5) Warman, J. M.; de Haas, M. P.; Dicker, G.; Grozema, F. C.; Piris, J.; Debije, M. G. *Chem. Mater.* **2004**, *16*, 4600.
- (6) McCulloch, I.; Heeney, M.; Bailey, C.; Genevicius, K.; MacDonald, I.; Shkunov, M.; Sparrowe, D.; Tierney, S.; Wagner, R.; Zhang, W.; Chabinyc, M. L.; Kline, R. J.; McGehee, M. D.; Toney, M. F. *Nat. Mater.* **2006**, *5*, 328.
- (7) (a) Mastalerz, M. *Angew. Chem., Int. Ed.* **2008**, *47*, 445. (b) Weder, C. *Angew. Chem., Int. Ed.* **2008**, *47*, 448.
- (8) (a) Côté, A. P.; Benin, A. I.; Ockwig, N. W.; O'Keeffe, M.; Matzger, A. J.; Yaghi, O. M. *Science* **2005**, *310*, 1166. (b) Côté, A. P.; El-Kaderi, H. M.; Furukawa, H.; Hunt, J. R.; Yaghi, O. M. *J. Am. Chem. Soc.* **2007**, *129*, 12914. (c) El-Kaderi, H. M.; Hunt, J. R.; Mendoza-Cortés, J. L.; Côté, A. P.; Taylor, R. E.; O'Keeffe, M.; Yaghi, O. M. *Science* **2007**, *316*, 268. (d) Uribe-Romo, F. J.; Hunt, J. R.; Furukawa, H.; Klöck, C.; O'Keeffe, M.; Yaghi, O. M. *J. Am. Chem. Soc.* **2009**, *131*, 4570.
- (9) (a) Furukawa, H.; Yaghi, O. M. *J. Am. Chem. Soc.* **2009**, *131*, 8875. (b) Doonan, C. J.; Tranchemontagne, D. J.; Glover, T. G.; Hunt, J. R.; Yaghi, O. M. *Nat. Chem.* **2010**, *2*, 235.
- (10) (a) Wan, S.; Guo, J.; Kim, J.; Ihee, H.; Jiang, D. *Angew. Chem., Int. Ed.* **2008**, *47*, 8826. (b) Wan, S.; Guo, J.; Kim, J.; Ihee, H.; Jiang, D. *Angew. Chem., Int. Ed.* **2009**, *48*, 5439.
- (11) (a) Fong, H. H.; Podzin, V. A.; Amassian, A.; Malliaras, G. G.; Smilgies, D.-M.; He, M.; Gasper, S.; Zhang, F.; Sorensen, M. *J. Am. Chem. Soc.* **2008**, *130*, 13202. (b) Guo, X.; Kim, F. S.; Jenekhe, S. A.; Watson, M. D. *J. Am. Chem. Soc.* **2009**, *131*, 7206. (c) Arias, A. C.; MacKenzie, J. D.; McCulloch, I.; Rivnay, J.; Salleo, A. *Chem. Rev.* **2010**, *110*, 3.
- (12) Van de Craats, A. M.; Warman, J. M.; Fechtenkötter, A.; Brand, J. D.; Harbison, M. A.; Müllen, K. *Adv. Mater.* **1999**, *11*, 1469.
- (13) (a) Pope, M.; Swenberg, C. E. *Electronic Processes in Organic Crystals and Polymers*; Oxford University Press: New York, 1999. (b) Das, A.; Dost, R.; Richardson, T.; Grell, M.; Morrison, J. J.; Turner, M. L. *Adv. Mater.* **2007**, *19*, 4018. (c) Andersson, L. M.; Osikowicz, W.; Jakobsson, F. L. E.; Berggren, M.; Lindgren, L.; Andersson, M. R.; Inganäs, O. *Org. Electron.* **2008**, *9*, 569.
- (14) Ding, X.; Guo, J.; Feng, X.; Honsho, Y.; Guo, J.; Seki, S.; Maitarad, P.; Saeki, A.; Nagase, S.; Jiang, D. *Angew. Chem., Int. Ed.* **2011**, *50*, 1289.
- (15) (a) Pisula, W.; Feng, X.; Müllen, K. *Chem. Mater.* **2011**, *23*, 554. (b) Boden, N.; Bushby, R. J.; Clements, J. J. *Chem. Phys.* **1993**, *98*, S920. (c) Simmerer, J.; Glösen, B.; Paulus, W.; Kettner, A.; Schuhmacher, P.; Adam, D.; Etzbach, K. H.; Siemensmeyer, K. J.; Wendorff, H.; Ringsdorf, H.; Haarer, D. *Adv. Mater.* **1996**, *8*, 815.